



ISSN: 2350-0328

**International Journal of Advanced Research in Science,  
Engineering and Technology**

Vol. 7, Issue 4, April 2020

# Magnetic materials synthesized in the sun furnace

Payzullakhanov Mukhammad-Sultan Saidvalikhanovich, Xolmatov Abdurashid Abdurakhim ugli, Sobirov Muslim  
Muhsinjon ugli

DSc, head of the laboratory for the synthesis and processing of materials of Institute of Material Science of SPA  
“Physics-Sun” AS RUz, Uzbekistan, Tashkent  
Assistant, Department of Informatics and IT, Fergana Polytechnic Institute, Uzbekistan, Fergana  
Assistant, Department of Informatics and IT, Fergana Polytechnic Institute, Uzbekistan, Fergana

**ABSTRACT:** The process of synthesis of materials in a solar furnace was studied using the example of ferrous barium oxide. It is shown that when  $\text{BaCO}_3 + \text{Fe}_2\text{O}_3$  is exposed to concentrated solar radiation of high ( $300 \text{ Wt/cm}^2$ ) density, hexagonal ferrous barium oxide  $4(\text{Fe}_2\text{O}_3)_4(\text{FeO})\text{BaFeO}_{3-x}$ , cubic  $\text{Ba}_3\text{Fe}_2\text{O}_{6-x} = 2(\text{BaO}) \text{FeOBaFeO}_{3-x}$ , tetragonal  $\text{BaOFeOBaFeO}_{3-x}$  modifications.

**KEYWORDS:** magnetic materials, coercive force, solar furnace, structure, magnetization.

## I. INTRODUCTION.

Depending on the microstructure, strontium and barium ferrites exhibit high values of electrical resistivity (not less than  $10^8 \text{ Ohm}$ ) and coercive force (not less than  $180 \text{ kA/m}$ ). Therefore, they are widely used to obtain permanent magnets. Having high magnetic energy ( $34 \text{ kJ/m}^3$ ) equal to alnico alloys, but with a low cost by an order of magnitude. Such features cause an increasing interest in barium and strontium ferrites[1].

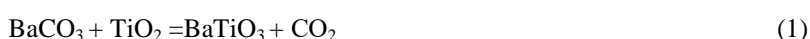
High-temperature ( $13500\text{C}$ ) ceramic technology is used to obtain strontium barium ferrites. In order to increase the level of properties, various technological modes are used, for example, activation of powders during grinding. [2]. Therefore, the question of modifying the composition and microstructure of barium and strontium ferrites using various methods of influencing raw materials in the synthesis of materials seems relevant.

The aim of this work was to study the synthesis of barium ferrite in a stream of concentrated high-density solar radiation.

## II. RELATED WORKS.

An important advantage of ceramics is the high availability of raw materials, including for the production of oxygen-free ceramics such as silicon carbides and nitrides, zirconium or aluminum, which replace scarce metals. Ceramics production, as a rule, does not pollute the environment to the same extent as metallurgy, and ceramic materials themselves allow the adoption of environmentally sound technological and technical solutions. The production of ceramics is usually safer than the production of alternative metal materials (due to the absence of electrolysis, pyrometallurgy, exposure to aggressive media), and ceramics with special properties can create effective fire-prevention systems. Ceramic samples of perovskites ( $\text{ABO}_3$ ) of barium titanate are obtained by the standard method of solid-phase reactions [3-10]. The kinetics of the formation during solid-phase synthesis of new structures is determined by: diffusion coefficients of atoms and their dependence on temperature, formation of phases of constant and variable composition in the reaction zone, etc. Unfortunately, despite studies of the physicochemical processes of the formation of oxide perovskites, a theoretical assessment of the necessary set of thermodynamic parameters for the successful synthesis of perovskites of any given composition has not yet been carried out. Most complex oxide materials are prepared by solid-phase technology in reactions of the oxide – oxide, oxide – hydroxide, or oxide – carbon – acid type [11].

$\text{BaTiO}_3$  ceramics are usually obtained by sintering at a high temperature of  $1573\text{--}1673 \text{ K}$  of an equimolecular mixture of  $\text{BaCO}_3$  and  $\text{TiO}_2$ . In this case, the following reaction occurs:





A more detailed description of the synthesis mode is given in [12-16]. Table 1 shows the structural parameters of the perovskite phases of BaTiO<sub>3</sub> formed after annealing at different temperatures. It can be seen that the low-temperature annealing of BaTiO<sub>3</sub> (up to 923 K) of the gel mixture leads to the formation of a cubic phase. Moreover, with an increase in the annealing temperature at room temperature, the value of the cell parameter decreases. Annealing in the temperature range 1023 K < T<sub>ann</sub> < 1473 K leads to the existence of a tetragonal BaTiO<sub>3</sub> phase at room temperature with an increase in spontaneous deformation (tetragonal distortion) with an increase in T<sub>ann</sub>, exhibiting an electric effect [17-23].

The above analysis shows that synthesis from the gas phase is based on condensation or chemical reactions of gas phase components, sol-gel synthesis in aqueous solutions is based on chemical reactions of exchange, decomposition, crystallization, and solid-phase reactions are based on diffusion at the interfaces. Each of these methods has its advantages and disadvantages, but none of them is universal. Therefore, one of the urgent problems of materials science, and in particular the synthesis of ferroelectric ceramics, is to study the processes of synthesis from the state of the melt obtained by exposure to concentrated solar radiation. A melt is a state of matter at temperatures close to the melting point. In contrast to ordinary liquids, the structure of melts contains crystal-like groups — associations, microcrystallites, the structure of which is associated with the structure of the crystalline phase. The technology of synthesis from the melt is based on the processes proceeding according to the following scheme: briquetting the initial mixture - melting on a solar furnace - quenching at a speed of 104-105 deg / s - grinding - sintering. The material obtained according to this scheme will exhibit enhanced mechanical and dielectric properties compared to those obtained by standard physicochemical and ceramic methods [24-28].

Table 1. Structural parameters of the perovskite BaTiO<sub>3</sub> phases formed after annealing at different temperatures

Material grade	Dielectric permeability	Curie Point, °C	Electromechanical coupling coefficient
TB-1	1500±300	110	0,20
TBK-3	1200±200	95	0,2
TBKC	450±50	150	0,17

### III. SIMULATION & RESULTS

A large number of physical methods of homogenization are known (the main of which in the technology of ceramic materials are dispersion and mixing of components in mills of various types). However, the most effective methods are chemical homogenization in the form of salts or hydroxides (coprecipitation, cryochemical synthesis, alkoxotechnology, etc.). Chemical homogenization of soluble metal compounds by transferring them to an aqueous or non-aqueous solution is one of the most universal methods for obtaining homogeneous salt precursors, since in this case a practically statistical distribution of cations is achieved. However, in the future, when extracting a solid from a solution, difficulties arise associated with incomplete or non-simultaneous deposition of individual components, different crystallization rates of substances, etc. When using synthesis from a melt, in most cases it is possible to significantly reduce the negative effect of these processes on obtaining a uniform composition final product.

To obtain ferrous barium oxide, the initial reagents used were barium carbonate BaCO<sub>3</sub> OSCh 9-3 TU 6-09-351-76, strontium carbonate BaCO<sub>3</sub> OSCh 7-2 TU 6-09-01-659-91, iron dioxide Fe<sub>2</sub>O<sub>3</sub> OSCh 2-4 TU 6-09-1418-78. The powders were mixed in the required proportion and briquetted.

Melting a mixture of iron oxide and barium carbonate on the focal plane of a solar furnace under the influence of a concentrated light flux of 350 W/cm<sup>2</sup> density with exposure to a melting state for 15 minutes. The melts were cooled in air (102 deg/s) and in running water (103 deg/s).

X-ray phase and X-ray diffraction analyzes of the studied samples were carried out on “DRON-3M” diffractometers (CuK $\alpha$  radiation). The radiation wavelength is  $\lambda = 0.193728$  nm. When recording the spectra of the samples, a Mn

filter was used. The focusing was carried out according to the Bragg-Bretano method with two Soller slots. The measurements were carried out at room temperature.

The resistivity was measured by the method of current-voltage characteristics and the two-probe method [29]. When conducting electrophysical measurements, copper contacts applied by sputtering at the VUP = 3 installation were used.

The magnetodielectric effect (MD effect, magnetocapacitance) was recorded by changing the dielectric constant when a sample was introduced into a magnetic field

$$\Delta(H)/\varepsilon(0) = (\varepsilon(H) - \varepsilon(0)) / \varepsilon(0)$$

where  $\varepsilon(H)$  and  $\varepsilon(0)$  – are the dielectric constant in the magnetic field and in its absence, respectively [30-32].

The magnetodielectric effect was recorded in a constant magnetic field of intensity  $H = 3.0$  kOe.

Figure 1. shows microscopic images of  $\text{BaCO}_3 + \text{Fe}_2\text{O}_3$  melts cooled a) in air (102 deg/s) and b) in running water (103 deg/s).

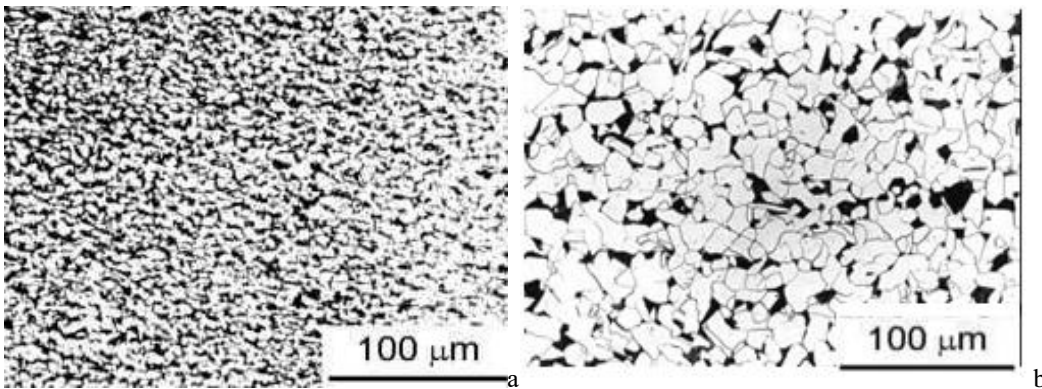


Figure 1. Microscopic images of  $\text{BaCO}_3 + \text{Fe}_2\text{O}_3$  melts cooled a) in air (102 deg/s) and b) in running water (103 deg/s).

An analysis of microscopic images showed that the melts consist of particles of various sizes and shapes. In the case of cooling in air, the morphology of the melt corresponds to a fine-grained structure with particle sizes of 1 -5 microns, and in the case of cooling in water - 10 - 20 microns.

Figure 2. shows X-ray diffraction patterns of  $\text{BaCO}_3 + \text{Fe}_2\text{O}_3$  melts cooled a) in air (102 deg/s), b) in running water (103 deg/s), c) annealed at a temperature of  $T = 1300^\circ\text{C}$ .

From the analysis of X-ray diffraction patterns of  $\text{BaCO}_3 + \text{Fe}_2\text{O}_3$  melts cooled a) in air (102 deg/s) and b) in running water (103 deg / s), it follows that depending on the cooling rate, material with varying degrees of amorphism can be obtained. Quenching in water allows you to fix the amorphous state of the substance. While cooling in air on the surface of a water-cooled substrate leads to a mixture of amorphous and crystalline phases - glassy material.

X-ray diffraction studies showed (Fig. 2) that the samples annealed at a temperature of  $T=1300^\circ\text{C}$  were polycrystalline and were a mixture of phases of ferrous barium of various modifications - hexagonal oxide of ferrous barium 4 ( $\text{Fe}_2\text{O}_3$ ) 4 ( $\text{FeO}$ )  $\text{BaFeO}_{3-x}$  with lattice parameters  $a = 5.86$ ,  $c = 23.2$  Å, cubic  $\text{Ba}_3\text{Fe}_2\text{O}_6-x = 2(\text{BaO}) \text{FeOBaFeO}_3-x$  with parameter  $a = 16.79$  Å, tetragonal  $\text{BaOFeOBaFeO}_{3-x}$  with parameters  $a = 5.98$ ,  $c = 13.93$  Å [30, 31].

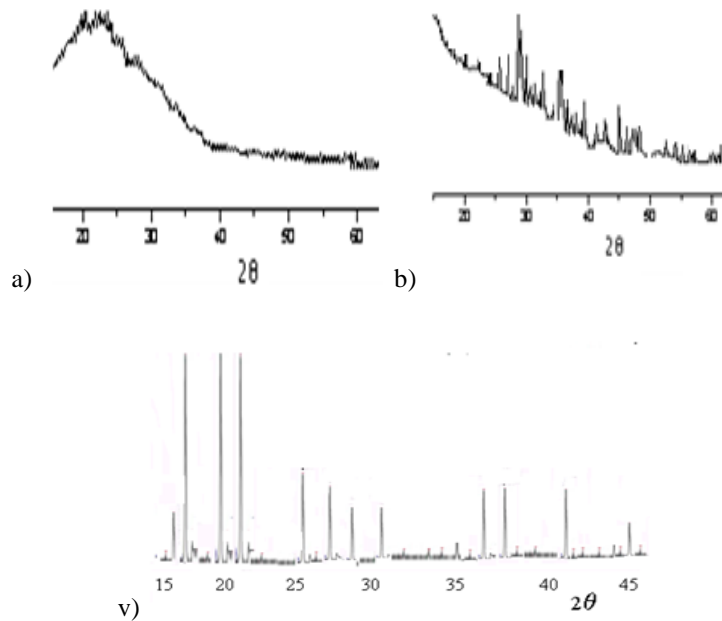


Fig. 2. X-ray diffraction patterns of BaCO<sub>3</sub> + Fe<sub>2</sub>O<sub>3</sub> melts cooled a) in air (102 deg / s), b) in running water (103 deg / s); c) calcined at a temperature of T = 1300°C.

Figure 3. shows the dependence of the dielectric constant of samples melted in a solar furnace and calcined at various temperatures.

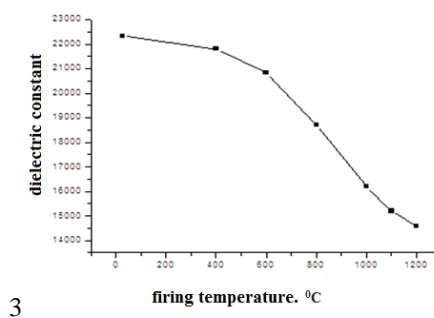


Fig. 3. The dependence of the dielectric constant of the A1-type samples, annealed at different temperatures.

It is seen that with an increase in the firing temperature, the dielectric constant decreases as compared to the fused sample.

Table 2 shows the results of LCR measurements of barium ferrite obtained under various technological conditions.

Table 2. LCR barium ferrite measurements

Samples	$\epsilon$	C, $\mu\Phi$
Water quenching	22340	920
Slow air cooling	19210	790
Sintered after hardening	14600	600
Solid Phase Synthesis in an Electric Furnace	7450	540

From table 2 it can be seen that high values of dielectric constant are observed in the case of quenching of the material melt in water. This is due to the fact that when melting on a solar furnace under the influence of concentrated solar radiation of high density, a large number of structural defects such as oxygen vacancies are formed mainly in the border regions, which lead to an increase in dielectric constant [32-36]. These defects are fired during thermal firing in air, and a decrease in the dielectric constant of the material is observed.

At the second stage of the experiments, the magnetic parameters of the samples were measured by the Weiss magnet method (Faraday scales) with a magnetic field of 3 kA.

Figure 4 shows the dependence of the interference on the balance on the distance from the center of the permanent magnet. When a sample is introduced into a magnetic field, as the sample approaches the center of the magnet, the interference on the balance grows. The magnetization curve is saturation.

When the sample is removed from the field of action of the magnet, the curve does not coincide. There is some hysteresis. There is a magnetization effect - residual magnetism appears. With subsequent inputs and outputs of the sample from the magnetic field, this difference disappears.

The Faraday scale makes it possible to estimate the magnetization of the material introduced into the magnetic field.

$$f \sim m\chi H \frac{dB}{dx}$$

From this we can obtain the expression for magnetic induction

$$\frac{\chi}{\mu_0} = \frac{f}{mB \frac{dB}{dx}}$$

where f is the interference on the scales, n; m is the mass of the sample, kg;  $\chi / \mu_0$  - specific magnetic susceptibility, N magnetic field strength, A / m; B - magnetic induction, T;  $\mu_0$  - magnetic constant  $\mu_0 = 4\pi \cdot 10^{-7}$  GN / m.

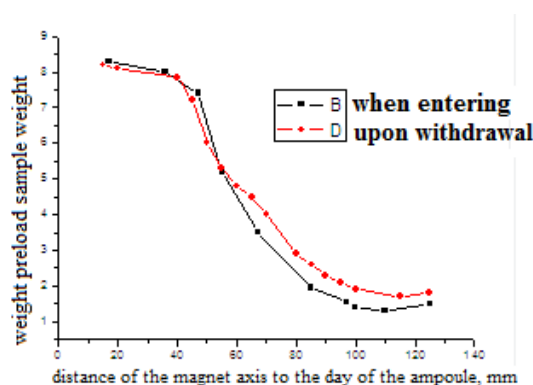


Fig. 4. The dependence of the interference on the scales from the distance from the center of the permanent magnet.

Table 3 shows the values of specific magnetization depending on the technological conditions of receipt.

Table 3. The values of specific magnetization depending on the technological conditions of receipt.

Material	$\frac{\chi}{\mu_0}$
Barium ferrite synthesized using a radiation heating unit without a magnetic field	350
Barium ferrite synthesized in a radiation heating apparatus in a magnetic field(3 kA/m)	360
Strontium ferrite synthesized in a radiation heating apparatus	360



in a magnetic field(3 kA/m)	
Bismuth ferrite synthesized in a radiation heating apparatus in a magnetic field(3kA/m)	260
BariumFerriteBrand 2BA2	240

Table 3 shows that barium, strontium and bismuth ferrites synthesized from a melt in a stream of concentrated light radiation are characterized by a 1.4-fold increase in the magnetization value compared to materials obtained by solid-phase synthesis, due to the microstructure of the material synthesized from a melt in solar ovens.

Based on the results obtained, it can be assumed that when a material is heated under the influence of concentrated light radiation due to intense absorption of concentrated solar radiation energy on structural defects at grain boundaries in a mixture of oxide materials, chemical reactions are initiated  $Fe_2O_3 + BaCO_3 = FeBaO_3 + CO_2$ .

#### IV. CONCLUSION

However, such processes occur at high speeds and thermodynamic conditions are rather far from optimal conditions typical for solid-phase synthesis. A high degree of defectiveness, both macroscopic (unlocking, dislocation, etc.) and microscopic (vacancies and other point defects), contributes to the destruction of the material. With increasing flux density, the processes of defect formation at the molecular level are accelerated due to the breakdown of chemical bonds and the loss of long-range order leading to melting.

According to the cluster model, the melt consists of clusters - crystal-like groups and an amorphous zone. An exchange of atoms takes place between clusters and disordered zones. Such an exchange becomes equilibrium at a constant temperature - the relative number of clusters and disordered zones does not change. With increasing temperature, the fraction of clusters decreases, and the fraction of a disordered zone increases.

The crystallization process during sintering of a glass powder obtained from a melt is accompanied by coagulation of clusters leading to the formation of crystalline nuclei and coagulation of nuclei leading to the formation of crystalline grains. Diffusion processes of atoms at grain boundaries, directed motion of point and extended defects to the grain surface, contribute to the coalescence of crystallites in the contact area. The disordered zone in the intergrain space due to surface tension forces limits the growth of grains during sintering.

These features of the microstructure determine the high permittivity and magnetization of glass-based materials obtained by exposure to concentrated light radiation. Such materials can be used in electronic devices.

#### V. THANKS

At the end of this research, we would like to sincerely thank to laboratory for the synthesis and processing of materials of Institute of Material Science of SPA "Physics-Sun" AS RUz. The work was carried out in the framework of the project of the Ministry of Innovative Development of the Republic of Uzbekistan № FI FA-F-3-02.

#### REFERENCES

- [1] [1] Permanent Magnets: A Guide. Под ред. Ю. М. Pyatina M.:Energy, 1980, - 488 c.
- [2] [2] Adamsov A.Yu. Obtaining and Properties of Hexagonal BaFe12O19 and BaFe12-xMxO19 Hexagonal Ferrites for Permanent Magnets and Substrates of Microwave Electronics Devices. Dis. Moscow 2016.210c.
- [3] [3] Gavrilova L.YA. Metodysintezaiissledovanieperspektivnyhmaterialov: Ucheb. posobie. – Ekaterinburg. Ural'skijgosudarstvennyjuniversitetim. A.M. Gor'kogo, 2008. – 402 s.
- [4] [4] Gromov O.G., Kuz'min A.P., Kunshina G.B., Lokshin E.P., Kalinnikov V.T. Poluchenieporoshko-obraznogotitanabariya // Neorganicheskimaterialy, 2006. – T. 42. – № 2. – S. 212-217.
- [5] [5] Cheng J.P., Agrawal D.K., Komarneni S., Mathis M., Roy R. Microwave processing of WC-Co composites and ferroictitanates // Mat. Res. Innovat. – 1997. – № 1. – Pr. 44-52.
- [6] [6] Vaidhyanathan B., Raizada P., Rao K.J. Microwave assisted fast solid state synthesis of niobates and titanates // J. Mater. Science Letters. – 1997. – № 16. – Pr. 2022-2025.
- [7] [7] Vaidhyanathan B., Anirudh P. Singh, Agrawal D.K. Microwave Effects in Lead Zirconium Titanate Synthesis Enhanced Kinetics and Changed Mechanisms // J. Am. Ceram. Soc. – 2001. – V. 84. – № 6. – Pr. 1197-1202.
- [8] [8] Pat. RF 2571478. Sostavkompozitsiidlyapolucheniya segnetoelektricheskogomaterialatitana-ta bariya-stronciya, gdepredlozhensostavdlyapolucheniya segnetoelektricheskogomaterialatitanabariya-stronciya / V.G. Baryshnikov, L.P. Efimenko, V.P. Afanas'ev.



ISSN: 2350-0328

# International Journal of Advanced Research in Science, Engineering and Technology

Vol. 7, Issue 4, April 2020

- [9] [9] Kim T.V. Sintezzol'-gel' metodomisvoystvatitanatabariya-stronciya-kal'ciyadlyaneohlazhda-emyh IK-priemnikov: Avtoref. diss.... kand. tekhn. nauk. 05.27.06. – Minsk, 2010. – S. 15.
- [10] [10] Pogibko V.M., Prisedskij V.V., Sidak I.L. Issledovaniemekhanizmovtermicheskogoraspada ok-salatnogoprekursoratitanatabariya // Voprosyhimiihimicheskoi tekhnologii. – 2010. – № 1. – S. 110-115.
- [11] [11] Baryshnikov V.G. Geterogennyevzaimodeystviya v processesintezatitanatovbariyaivismuta v rasplavahsolej: Diss... kand. him. nauk. – Sankt-Peterburg, 2009. – 150 s.
- [12] [12] Ivanov K.V. ZHidkofaznyjsintezacetato-, oksalato- igidroksotitanilovnekotoryh nS2 me-tallov, fiziko-himicheskiesharakteristikihtermicheskikhprevrashchenijielektroreologicheskiesvojstva: Diss... kand. him. nauk. – Ivanovo, 2011. – 150 s.
- [13] [13] SHut V.N., Kostomarov S.V. Zavisimost' svoystvporoshkovtitanatabariyaotrezhimatermo-obrabotkititaniloksalatabariya // Neorganicheskiesmaterialy. – 2012. – T. 48. – № 6. – S. 706-712.
- [14] [14] CHuppina S.V., ZHabrev V.A. Izmenenienergeticheskikhharakteristikpoverhnostiorganosili-katnyhpokrytij v processeformirovaniya // Fiz. i him. stekla. – 2007. – T. 33. – № 6. – S. 872-883.
- [15] [15] Ivanov K.V., Agafonov A.V., Zaharov A.G. Zol'-gel' sinteznanorazmernihacetatotitanilovbariya, bariya-stronciyaibariya-kal'ciya: termicheskayaevoluyuciya v titanaty // Izvestiyavuzov: «Himiyaihimicheskietekhnologii», – 2010. – T. 3. – № 12. – S. 74-78.
- [16] [16] Agafonov A.V., Ivanov K.V., Davydova O.I., Kraev A.S., Trusova T.A., Zaharov A.G. ZHidkofaznyjsintezsolejacetato-oksalatotitanilbariyakakintermediatovdlyapolucheniyananorazmernogotitanatabariya // ZHurn. neorg. himii, – 2011. – T. 56. – № 7. – S. 1087-1091.
- [17] [17] ZHabrev V.A., Efimenko L.P., Baryshnikov V.G., Polyakova I.G., Gumennikov A.V. Sintezporoshkov BaTiO3 raznojdispersnostiputemobmennyhreakcij v rasplavah. / Fiz. i him. stekla. – 2008. – T. 34. – №1. – S. 116-123.
- [18] [18] Pat. RF 2374207, MPK C04V35/475. Sostavkompozitsiidlyapolucheniya segnetoelektricheskogomateriala / V.A. ZHabrev, L.P. Efimenko, V.G. Baryshnikov, V.P. Afanas'ev. Opubl. 27.11.2008.
- [19] [19] Mihajlov M.M., Sokolovskij A.N. Sintezisvoystvsoedinenij BaSrTiO3 // DokladyTUSURa – Dek., 2007. – № 2(16). – S. 198-203.
- [20] [20] Rout S.K., Panigrahi S. Mechanism of phase formation of BaTiO3 – SrTiO3 solid solution through solid oxide reaction // Indian journal of pour and applied physics. – 2006. – V. 44. – Rp. 608-611.
- [21] [21] Mitoseriu L., Tura V. Razmerzernovyhzavisimyhtermicheskikhgisterezisov v keramiketitana-tov bariya // Analestintifice ale universitatii «al.i.cuza» din iasi. – Tom. XLI-XLII s.Ib.fasc.2 FizicaSolidelor – FizicaTeoretica. – 1998-1999. – Pr. 113-124
- [22] [22] Dzhabarov S.G. Kristallicheskayastrukturatitanabariyaprizvozhdeystviidavleniyaitemperatury // Uspekhhifizikimetallov. – 2015. – T. 16. – S. 329-352.
- [23] [23] Payzullahanov M.S. Particularities of the syntheses BaTiO3 in the field of concentrated light energy // Horizon Research Publishing. – USA Manuscript. ID:16200286. – 2013. – № 27.
- [24] [24] Pajzullahanov M.S., NurmatovSH.R.,SHermatov ZH.Z. Titanatybariyaistronciya, sinteziro-vannye v pole koncentrirovannojsvetovojenergii // Stekloikeramika. – 2013. – № 6. – S. 123-125.
- [25] [25] Pajzullahanov M.S., FajzievSH.A.,Nurmatov SH.R., SHermatov ZH.Z. Osobennostisintezati-tanatabariya v pole koncentrirovannojsvetovojenergii // Geliotekhnika, – 2013. – № 4.
- [26] [26] R.Y.Akbarov, M.S.Paizullakhanov. Characteristic features of the energy modes of a large solar furnace with a capacity of 1000 kW// Applied Solar Energy, v.54. #2. pp.99-109.(2018)
- [27] [27] A.Abdurakhmanov, Sh.Faiziev, R.Akbarov, S.Suleimanov, M.Rumi, M.S Paizullakhanov, E.Nodirmatov. Properties of pyroxene glass ceramics, heat treated in the Big Solar Furnace// Applied Solar Energy, v.45. #1. pp.45-47. (2009)
- [28] [28] Rovin S.V. Vliyaniedispersnostimaterialovnaskorostiprocessovtverdogofaznogovosstanovle-niya // Lit'eimetallurgiya, – 2014. – T. 4. – № 77. – S. 7-9.
- [29] [29] Pyatakov A.P., Zvezdin A.K. Magnetolectric materials and multiferroics. //UFN. -2012. T.186. №2. C.593-620.
- [30] [30] Amirov A.A., Batdalov A.B., Kallayev S.N. and other. Features of the thermal, magnetic and dielectric properties of multiferroics BiFeO3 и Bi0.95La0.05FeO3 // ФТТ. - 2009. Т. 51. Вып. 6. С. 1123-1126
- [31] [31] Wang J., Neaton J.B., Zheng H. et. al. Epitaxial BiFeO3 Multiferroic Thin Film Heterostructures// Science.- 2003. Vol. 299. P. 1719-1722.
- [32] [32] Abdurakhmanov A.A., Faiziev S.A., Akbarov R.Y., Suleimanov S.K, Rumi M.K. Properties of pyroxene glass ceramics, heat treated in the Big Solar Furnace//Applied Solar Energy 45 (1), 45-47
- [33] [33]Paizullakhanov M.S., Faiziev S.A., Nurmatov S.R. Synthesis features of barium titanate in the field of concentrated light energy//Applied Solar Energy 49 (4), 248-250
- [34] [34] Abdurakhmanov A.A., Paizullakhanov M.S., Akhadov Z. Synthesis of calcium aluminates on the big solar furnace Applied Solar Energy 48 (2), 129-131
- [35] [35] Akbarov R.Y., Paizullakhanov M.S. Characteristic Features of the Energy Modes of a Large Solar Furnace with a Capacity of 1000 kW//Applied Solar Energy 54 (2), 99-109
- [36] [36]Abdurakhmanov A.A., Paizullakhanov M.S., Akhadov Z. Synthesis of calcium aluminates on the big solar furnace//Applied Solar Energy 48 (2), 129-131.